JOURNAL OF AGRICULTURAL AND FOOD CHEMISTRY

Article

pubs.acs.org/JAFC

Interfacial Study of Class II Hydrophobin and Its Mixtures with Milk Proteins: Relationship to Bubble Stability

Yiwei Wang,[†] Cédric Bouillon,[†] Andrew Cox,[‡] Eric Dickinson,[†] Kalpana Durga,[†] Brent S. Murray,*[,†] and Rong Xu[†]

[†]Food Colloids Group, School of Food Science and Nutrition, University of Leeds, Leeds LS2 9JT, United Kingdom

[‡]Unilever Research and Development, Colworth Science Park, Sharnbrook MK44 1LQ, United Kingdom

Supporting Information

ABSTRACT: Class II hydrophobin (HFBII) is a very promising ingredient for improving food foam stability. Pure HFBII-stabilized bubbles exhibited exceptional stability to disproportionation (dissolution) but were not stable to bubble coalescence induced by a pressure drop. Bubbles stabilized by mixtures of HFBII + sodium caseinate (SC) or β-lactoglobulin (BL) showed decreased shrinkage rates compared to pure SC or BL and improved the stability to pressure-drop-induced coalescence. Higher bubble stability was more closely correlated with higher surface shear viscosity than the surface dilatational elasticity of the mixed protein systems. Brewster angle microscopy observations and the high shear strength of adsorbed films, including HFBII, even in the presence of hydrophobic and hydrogen-bond-breaking agents, confirm that intermolecular attractive cross-links are unlikely to be the origin of the high strength of HFBII films. Possibly the HFBII molecules form a tightly interlocking monolayer of Janus-like particles at the air−water interface.

KEYWORDS: *Hydrophobin, bubble, foam, protein, interfacial rheology*

INTRODUCTION

One way of creating extremely stable bubbles is to surround them with an adsorbed layer of solid particles instead of using surface-active macromolecules or low-molecular-weight surfactants. The underlying concepts and theory relating to bubble stabilization by particles have been reviewed in the literature.[1−3] In practice, however, finding surface-active particles that are non-hazardous and in the correct size range for stabilizing aerated food systems is difficult.[2] The fungal protein hydrophobin may fulfill these food acceptability criteria,[4] because this unusual protein can adsorb and behave like a rigid hydrophobic Janus-type particle.[5]

Linder[6] has recently provided a comprehensive review of the structure and properties of hydrophobins, produced by filamentous fungi. At a hydrophilic−hydrophobic interface, hydrophobins spontaneously self-assemble into an amphiphilic membrane.[7] According to their solubility properties, hydrophobins are divided into two groups. The class I hydrophobins form highly insoluble membranes that can only be dissolved with certain strong acids, whereas the class II hydrophobins (HFBIIs) can be readily dissolved in ethanol, sodium dodecyl sulfate (SDS),[13] or water. Hydrophobins can change the nature of a surface, via self-assembly, from hydrophobic to hydrophilic or vice versa. These properties therefore make class I hydrophobins suitable for modifying solid surfaces, while attention toward HFBIIs has been directed more to use in liquid systems.[8] Indeed, HFBIIs have been found to be too efficient as foam-forming or bubble-nucleating agents, causing beer foam to gush upon opening the bottle.[9] However, HFBIIs were not studied in detail from the surface chemistry point of view until the work by Cox et al.[5,10] Another reason for investigating HFBII for use in foods rather than the class I hydrophobins is that they can be produced at relatively high yield levels.[8] The HFBII produced by *Trichoderma reesei* was used in the experiments described in this paper.

HFBII has a molecular weight of about 7 kDa. The common structural feature of HFBII and the other hydrophobins is the presence of eight conserved cysteine residues in the amino acid sequence.[11] The crystal structure of HFBII, with a patch of hydrophobic side chains located on the protein surface, is the key feature contributing to its amphiphilicity.[7] The size of the hydrophobic patch was estimated to be from 12 to 19% of the total surface area of the protein.[7] The patch gives the "surface" of the molecule two types of "faces", hydrophilic and hydrophobic, like so-called Janus colloidal particles. Fibrillar aggregates appear in bulk solution upon shaking, and monoclinic and orthorhombic crystal structures of these aggregates have been described, where it is suggested that the hydrophobic sides of adjacent molecules are aligned within the self-assembled structures.[7] Hakanpaa et al.[11] proposed a model of HFBII multimerization in solution and monolayer formation at the air−water (A−W) interface. In bulk solution, HFBII usually exists in a tetramer state, with the hydrophobic patches of the molecules concealed inside the tetramer. These low-molecular-weight aggregates more favorably form monolayers of hexagonally ordered two-dimensional crystallites of various types[12] at an interface between two phases of different polarity, exposing the hydrophobic side toward the more hydrophobic phase. This process of concealing the hydrophobic patch from

Received: October 28, 2012
Revised: January 21, 2013
Accepted: January 24, 2013
Published: January 24, 2013

the more polar phase as the driving force for self-assembly is commonly accepted in the literature.[13−17] However, on the basis of film-thinning measurements, Basehva et al.[18] recently suggested that dimers and tetramers can also attach to bubble surfaces via aggregation of their hydrophilic faces, although the exact mechanism of the hydrophilic interaction was not clear. Recent non-invasive studies of the structure of hydrophobin molecules adsorbed at the A−W interface[19] and in the bulk solution[20] via neutron reflectivity and small-angle neutron scattering, respectively, have confirmed most of these features of adsorption while also highlighting that even low-molecular-weight surfactants can only displace HFBII at relatively high concentrations. Concentrations above the surfactant critical micelle concentration are required, although this is complicated by the formation of complexes between HFBII and the surfactant molecules.

All in all, the self-assembly properties and surface activity of hydrophobins make them promising for various applications, including foam stabilization. Recently, for example, Tchuenbou-Magaia et al.[21] have proposed using hydrophobin-stabilized bubbles as inclusions within oil-in-water emulsions as a fat replacer. However, a proper explanation of the unusual surface rheological behavior of HFBII would help to explain its foam-stabilizing properties more fully. For example, although lateral interactions between the adsorbed molecules have been proposed as promoting the high degree of ordering of the films, the nature of these lateral interactions has thus far avoided identification.[6,22] Furthermore, from a practical point of view, mixtures of hydrophobin with other commonly used foaming agents should also be tested for more direct relevance to real food systems, where other components will be present. In particular, it is of interest to know whether HFBII is able to maintain its functionality within a complex food foam system containing other surface-active proteins and ingredients or, better still, whether synergistic effects can occur with these other components that give better foamability and foam stability overall. The majority of foamed food products, apart from beverages, are dairy-based, and therefore, the possibility of exploiting the benefits of HFBII in such products is of interest. Therefore, in this paper, in addition to testing HFBII on its own in terms of bubble coalescence stability, disproportionation and surface rheology, it is studied in admixture with two major milk protein fractions that have been tested similarly previously:[23,24] sodium caseinate (SC) and the whey protein β-lactoglobulin (BL).

MATERIALS AND METHODS

Materials and Sample Preparation. HFBII (0.435 wt %) was supplied by VTT Biotechnology (Espoo, Finland) and prepared as previously described.[25,27] The HFBII was supplied in an ammonium acetate buffer solution. This solution was freeze-dried and stored at 40 °C in a vacuum oven for 18 h to remove water and buffer, to enable solutions be prepared at different pH values. HFBII was then reconstituted in pure water at a concentration of 0.5 wt % and stored frozen. Before conducting a new measurement on each sample, a 2 min period of sonication at 45 kHz (Kerry sonicator, Kerry Ultrasonics, Hitchin, Herts, U.K.) was applied separately to the original 0.5 wt % solution and also to the diluted sample. This step is necessary to remove any small bubbles and to dissociate any protein aggregates. Spray-dried SC (>82 wt % dry protein, <6 wt % moisture, <6 wt % fat and ash, and 0.05 wt % calcium) was supplied by DMV International (Veghel, The Netherlands). Bovine BL (3 times crystallized, lyophilized, and desiccated, lot number 21K7079, containing variants A and B), sodium thiocyanate, SDS, potassium dihydrogen phosphate, disodium hydrogen phosphate, and urea were purchased from Sigma-Aldrich (Poole, U.K.). All solutions were prepared using Milli-Q water (Millipore, Watford, U.K.), which is free from surface-active impurities and with a conductivity of less than 10^{-7} S cm^{-1}. Aqueous solutions of SC and BL (1 or 2 wt %) were prepared by dispersing the required amount of protein in Milli-Q water under gentle stirring for 4 h at room temperature. The appropriate concentration of protein for experiments was then created by diluting these aqueous solutions into pH 7 phosphate buffer. All experiments were carried out at 25 °C and pH 7, unless stated otherwise.

Apparatus. The bubble coalescence cell and its operation have been described in detail previously,[24,26] and only brief information is given here. A flexible square barrier is positioned at the A−W interface of the aqueous solution contained within a specially designed cell. The barrier can be expanded or compressed, and the air pressure above the interface simultaneously decreased or increased, respectively. Bubbles with a typical size range of 100−300 μm diameter are injected into the cell. Bubbles were created by either injecting air through a specially designed syringe[26] or injecting preformed bubbles, formed via aeration in a food blender of the same solution as in the cell, via a plastic pipet. A side arm in the cell allows for injection, via the syringe or pipet, beneath the A−W interface. It typically takes 1−2 min to inject a sufficient number of bubbles beneath the interface for a single experiment. After this time, resistance to coalescence with the planar interface is tested by lowering the air pressure and expanding the barrier to expand the bubbles and the planar interface, such that the bubbles undergo the same rate and extent of area expansion as the planar interface. The bubbles are observed from above via a microscope, and the sequence of events is digitally recorded. The number fraction of bubbles that are stable to coalescence on expansion, F_s, is determined from the recording. Experiments were carried out at least 3 times, and the variation about the mean F_s values was <0.05. The technique has been shown to be highly effective in discriminating the abilities of different proteins, etc., to stabilize bubbles against coalescence, and it has shown good correlation with measurements of bulk foam stability.[24,26,28]

Absolute surface tension was determined using a Krüss KT-10 digital tensiometer (Krüss USA, Charlotte, NC) equipped with a vertically suspended platinum Wilhelmy plate, operating in detachment mode. Experiments were carried out at least 3 times, and the variation about the mean surface tension was <0.5 mN m^{-1}. To measure the surface shear viscosity of the adsorbed films, a two-dimensional Couette-type interfacial viscometer[29,30] was operated in a constant shear rate mode. A biconical disk is suspended from a torsion wire with its edge at the A−W interface of the solution contained within a cylindrical dish. The constant shear rate apparent surface viscosity, η_s, is given by the equation

$$\eta_s = \frac{g_f}{\omega} K(\theta - \theta_0) \quad (1)$$

where K is the torsion constant of the wire, θ is the equilibrium deflection of the disc in the presence of the film, θ_0 is the equilibrium deflection in the absence of the film, i.e., because of the bulk drag of the subphase on the disk, g_f is the geometric factor, and ω is the angular velocity of the dish. A fixed value of $\omega = 1.27 \times 10^{-3}$ rad s^{-1} was employed throughout, to facilitate comparison to measurements reported previously.[29,30] Experiments were carried out at least 3 times, and the variation about the mean η_s was <0.1 N s m^{-1}.

A Langmuir trough with a flexible square rubber barrier was used to measure the dilatational rheology of the adsorbed films. The essential details of the apparatus have been described by Xu et al.[31] The only difference here compared to the setup used by Xu et al.[31] is that a larger barrier and trough were used for a greater range of expansion and contraction of the film area. The inside dimensions of the trough were 14.3 cm^2, and the rubber barrier was able to expand from 4.5 to 12 cm^2. After filling the trough to the required level with the aqueous phase, the surface was aspirated away via a clean Pasteur pipet and vacuum pump. The interface was then left for 2 min before suddenly expanding the interface and recording the change in surface tension ($\Delta\gamma$) with time. The 2 min waiting time was to match, as far as

possible, the time taken to inject bubbles beneath the planar interface in the bubble coalescence cell. The planar interface in the trough was subjected to the same rate of area strain, $d \ln A/dt$, and the same relative increase in area, A/A_0 (where A_0 and A are the initial and final areas, respectively), as the bubbles and planar interface in the coalescence cell. Further details are given elsewhere.[28] As in our previous work,[28,31−33] it was found that the initial gradient of the $\Delta\gamma$ versus $\ln A$ curve was a convenient measure of the dilatational rheological response of the films. The $\Delta\gamma$ versus $\ln A$ data over the first 5% of the total time of the expansion period were fitted to a straight line, and the gradient of this line was termed the "average initial dilatational elasticity", ϵ^*_{init}. This is really a complex modulus. A further justification for analyzing the data in this way is that, when bubble coalescence occurs in the pressure drop test, it tends to do so more at the start of the expansion. The fit to a straight line was always good enough to give a regression coefficient >0.97. Experiments were carried out at least 3 times, and the variation about the mean ϵ^*_{init} value was <4 mN m^{-1}.

Images of adsorbed protein films at the A−W interface were recorded using a BAM2plus Brewster angle microscope (NFT, Gottingen, Germany), fitted with a similar but smaller Langmuir trough, as described elsewhere.[32] All experiments were carried out at 20 ± 3 °C, and all images were collected from the center of the rubber barrier.

RESULTS AND DISCUSSION

Brewster Angle Microscopy (BAM). Representative BAM image sequences of the adsorbed film behavior of HFBII during interfacial expansion and compression are shown in Figures 1 and 2. BAM creates an image from the reflection of a *p*-polarized laser light beam scanned over the interfacial film. The reflected intensity increases with increasing optical density and/or thickness of the protein film, while areas of no film appear black, i.e., zero reflected light. Figure 1A shows features therefore corresponding to HFBII aggregates, i.e., bright specks, that appeared at the surface (0.25 h) after the new interface was formed from adsorption from a bulk protein concentration (C_b) = 10^{-2} wt % HFBII. After 0.5 h (Figure 1B), there was an insignificant increase in the surface density of these aggregates. The aggregates were distributed randomly in the interface and did not drift >10 μm in 1−5 s, suggestive of a high viscosity film, although they did move at the extremes of the area compression and expansion. Expansion of the film by a factor of 3, i.e., A/A_0 = 3, decreased the surface density of the aggregates (Figure 1C). Recompression of this expanded film to its original area caused more densely packed material to appear at the surface (Figure 1E), as indicated by the brightness of the structures and the striations within them. Each expansion and compression stage took approximately 20 s. The striations are indicative of folds or ridges within the adsorbed film. This suggests that, in the time in which it took to perform the expansion and compression, plus the time taken to acquire the images (approximately 5 min), considerable further adsorption of HFBII occurred at the interface, such that, upon recompression, saturation coverage was reached and also that HFBII desorption did not readily occur. However, this was expected from the known high surface activity of HFBII and the C_b used in these experiments. Intriguingly, on re-expansion again to A/A_0 = 3 (Figure 1F), the dense structures observed immediately before re-expansion (Figure 1E) broke up readily, indicating that no strong permanent cross-linking had occurred in the densely packed film.

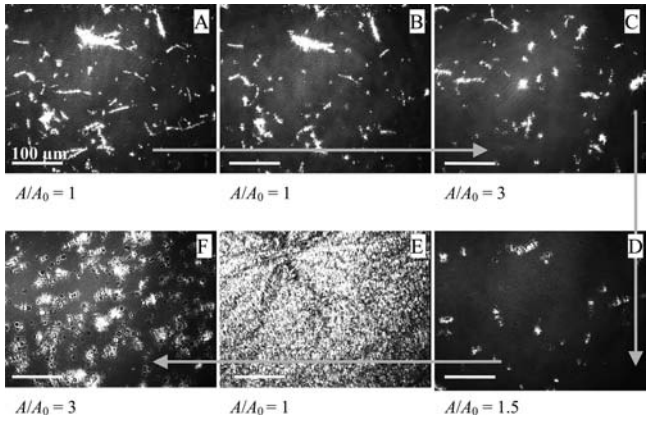

Figure 1. BAM image sequence (A → F) for the A−W interface of C_b = 10^{-2} wt % HFBII subjected to different expansion and compression. Freshly made film is over a short time scale of 0−0.5 h. The size bar = 100 μm. The gray arrows indicate the sequence of compression/expansion. A/A_0 is the ratio of the film area to the initial film area.

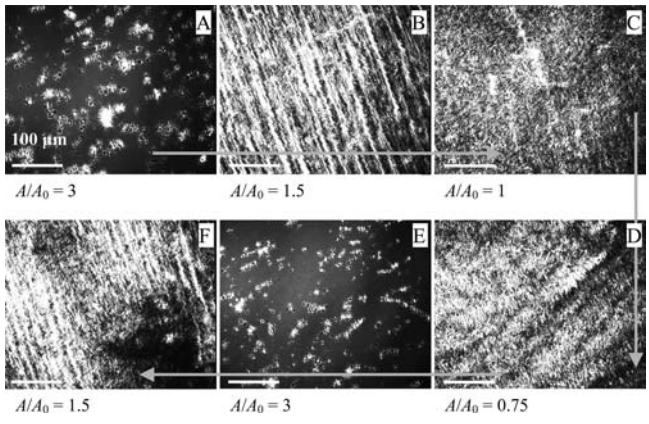

Figure 2. BAM image sequence (A → F) for the A−W interface of C_b = 10^{-2} wt % HFBII subjected to different expansion and compression, for a 4-h-old film. The size bar = 100 μm. The gray arrows indicate the sequence of compression/expansion. A/A_0 is the ratio of the film area to the initial film area.

Figure 2 shows images of the same film as in Figure 1 but beginning (Figure 2A) after holding at A/A_0 = 3 until a total film age of 4 h. Over this extra adsorption time, few further changes occurred (compare Figures 1F and 2A). However, upon compression of the film to A/A_0 = 1.5 (Figure 2B) and then A/A_0 = 1 (Figure 2C), more highly structured films were observed than for the 0.5-h-old film shown in Figure 1. Basheva et al.[18] recently published similar optical images of the surface of shrunken bubbles stabilized by HFBII, obtained via conventional light microscopy, while Blijdenstein et al.[34] also observed such structures for spread monolayers of HFBII. It was surprising that, upon subsequent re-expansion to A/A_0 = 3 (Figure 2E), all of this structure also disappeared immediately, although it started to reappear upon further compression (Figure 2F). The same sort of pattern of behavior in the film structure was observed for a film adsorbed from the same C_b but aged for 22 h when subjected to similar cycles of expansion and compression (see the Supporting Information). After 22 h, the structures formed upon compression were even more pronounced than for the 4-h-aged film, but upon re-expansion, these again disappeared immediately.

Overall, the BAM observations suggest rapid and extensive adsorption of HFBII to give a close packed film that becomes even more close packed upon compression, such that it buckles

and folds. However, there is no permanent attractive cross-linking induced between the film components, because the condensed film rapidly redisperses upon expansion of the interface. These observations are consistent with previous investigations,[5,7,11,22] which also suggest that the HFBII molecules behave like strongly adsorbing hard particles, which is also the main conclusion of the spread monolayer work by Blijdenstein et al.[34] The small rigid molecules adsorb to the surface strongly because of their hydrophobic patches and do not form multilayers or exhibit displacement back into the bulk when the layers are compressed. Rather, the adsorbed film buckles upon compression. However, because there is negligible protein unfolding upon adsorption[35] and no establishment of strong irreversible attractive interactions between the adsorbed HFBII molecules, the films dissociate easily upon re-expansion. Aumaitre et al.[36] have reported results on spread monolayers of hydrophobin suggesting that condensed and dilute HFBII domains might coexist, explaining a sharp increase in viscoelasticity of the monolayers still at low surface pressures. At least at the resolution of the BAM, we see negligible evidence of extensive condensed domains upon re-expansion of the adsorbed films. However, interlocking of coherent domains (rather than molecules) possibly contributes to the high surface shear viscosity of adsorbed HFBII films.

Pressure-Induced Coalescence of Bubbles. Cox et al.[5,10] have reported that an aqueous solution of HFBII is very easy to foam via whipping. However, under the methods and conditions adopted in our work, using a needle or bubble syringe[26,37] to inject bubbles beneath the planar A−W interface, it was difficult to obtain a high proportion of bubbles that did not coalesce immediately upon reaching the planar interface. Those bubbles that were stable were relatively large (e.g., bubble diameter ≈ 500 μm). Thus, the initial adsorption of HFBII to the bubbles under quiescent conditions did not result in an adsorbed film readily capable of preventing coalescence, in contrast to the other proteins tested previously.[26] On the other hand, it is reported that vigorous shearing methods with HFBII can produce very small and stable bubbles[5,9] compared to milk proteins. This is probably because the intense shear forces increase the mass transport of HFBII molecules or their aggregates to the interface. Alternatively, the adsorbed films formed under shear may have different properties compared to those formed solely via molecular diffusion under quiescent conditions. In fact, shearing promotes the formation of aggregates of HFBII in the bulk solution,[5,38] possibly via desorption and rearrangement of fragments of monolayer transiently formed at the interface under dynamic conditions. Thus, the formation and adsorption of aggregates at the interface may explain the better foam properties under shearing conditions. Nevertheless, some experiments on coalescence toward an applied pressure drop could be performed on the small numbers of bubbles that were stable before expansion of the A−W interface.

Figure 3 shows the fraction of bubbles stable to pressure-induced coalescence (F_s) for $C_b = 10^{-2}$ wt % HFBII as a function of their initial bubble diameter (i.e., before their expansion). Because it was not possible to control the exact bubble size distribution of bubbles injected, F_s values have been averaged for the same values of bubble diameter ±5 μm. It should be noted that all of the bubbles present at the start of the experiment were completely stable to coalescence in the absence of the pressure-induced expansion. Figure 3 shows that >90% of the HFBII-stabilized bubbles were quite unstable to

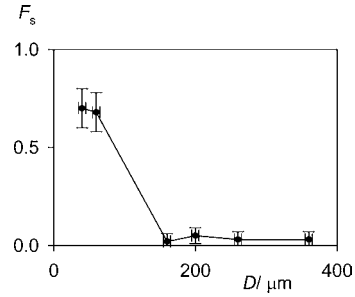

Figure 3. Number fraction (F_s) of bubbles stable to pressure-induced coalescence for $C_b = 10^{-2}$ wt % HFBII as a function of the bubble diameter (D). Each data point is the average of three sets of experimental results, with the error bars equal to the maximum variation about the mean.

expansion; i.e., F_s was <0.1 for bubble sizes above 150 μm, although the smaller bubbles (diameter ≈ 50 μm) were more stable ($F_s \approx 0.7$). With other proteins, it has also been observed that larger bubbles are less stable to pressure-induced coalescence, probably because of the size-dependent buoyancy forces. However, the effect of the bubble size with these proteins, which included BL, whey protein isolate, SC, ovalbumin, and gelatin, were not so extreme as noted here for HFBII, so that all of the HFBII-stabilized bubbles were considerably less stable than similar size bubbles stabilized by other proteins under similar conditions of expansion.[24,26]

The pressure-induced coalescence stability of systems containing both 10^{-2} wt % HFBII and SC or BL was also measured. SC and BL were added at a higher concentration, C_b = 0.3 wt %, because HFBII is more surface-active than both of these proteins, and therefore, a higher concentration should be required to allow for the milk protein to compete with HFBII at the interface. F_s was determined for bubbles in the size range of 150−250 μm. Considering the reproducibility in the F_s measurements (±0.05) and the mostly low (<0.1) values of F_s with HFBII alone, the mixed SC system had similar stability to SC on its own: for the HFBII + SC mixture, F_s = 0.55 compared to F_s = 0.52 for SC alone. For the HFBII + BL mixture, F_s = 0.74 compared to F_s = 0.33 for BL alone. Thus, HFBII does not compromise the stabilizing effects of SC and BL, at least at this concentration (10^{-2} wt %), and for BL, there is actually some improvement, which is noteworthy because BL is even less surface-active than SC. At present, the origin of this enhancement is unknown: all three proteins have net charges of the same sign (negative) at pH 7; therefore, any interaction seems unlikely to be electrostatic in nature.

The effect of hydrophobic bonds on the bubble stability was also investigated. The hydrophobic patch on the HFBII molecule may be one way in which it could form attractive interactions with other protein molecules at the interface and affect adsorbed film properties. The β- and α_{s1}-casein components of SC have particularly open hydrophobic domains that could allow for this sort of interaction, while it is less likely for BL, which is a typical globular protein, with the hydrophobic domains largely buried in its the interior. The hydrophobic bond breaking agent, NaSCN, was introduced at a concentration of 0.5 mol dm^{-3} to a mixed solution of C_b = 0.3 wt % SC + 10^{-2} wt % HFBII, and the pressure-induced coalescence stability was measured as above. The inclusion of NaSCN had a minor effect: the value of F_s = 0.63 was almost the same as the value (F_s = 0.55) in this system without NaSCN. Consequently, these experiments provided no

evidence of hydrophobic bonding between SC and HFBII enhancing stability.

Disproportionation of Bubbles Stabilized by Hydrophobin. It is already known that HFBII-stabilized bubbles are very stable to disproportionation.[5,10,34] This is confirmed in Figure 4, even under the conditions of low C_b (10^{-2} wt %) for

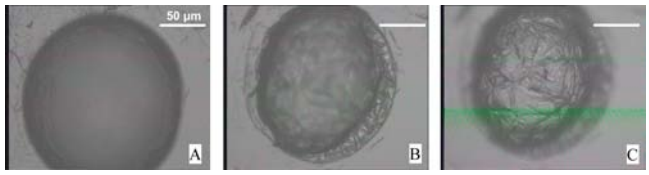

Figure 4. Light microscope images showing the age-induced shrinking effects for air bubbles stabilized by $C_b = 10^{-2}$ wt % HFBII. Image A shows a freshly produced bubble, with the focusing level exactly at the A–W interface. Images B and C show the same bubble as in image A after 4 days of aging under atmospheric pressure, with the focusing level at the A–W interface and slightly above the interface, respectively. The size bar = 50 μm.

HFBII. Figure 4 shows representative images of bubbles injected beneath the planar interface in the coalescence cell but when no pressure change was applied. Figure 4A shows the wrinkled "skin" on a freshly injected bubble. After 4 days of storage, images B and C of Figure 4 show that there was less than 10% shrinkage in the size of this bubble, which retained its former shape, with the original boundary of the bubble still being distinguishable. The wrinkles at the bubble surface are similar to those observed in the BAM images for the compressed adsorbed films at the planar A–W interface. In the case of a spherical bubble stabilized by HFBII, although the Laplace pressure drives disproportionation to take place to a small extent initially, the mechanically strong wrinkled structure clearly resists further shrinkage. However, when such a bubble is subjected to an expansion, film rupture and bubble coalescence readily occur, and this observation fits in with the ready disappearance of the wrinkles, etc., upon expansion of the films in the BAM experiments.

Disproportionation of Bubbles Stabilized by Hydrophobin + Milk Proteins. Previous studies[39] have shown that milk proteins do not confer good stability against disproportionation of air bubbles, whereas the results above show that hydrophobin can form adsorbed films that give strong resistance to bubble shrinkage. The disproportionation behavior of mixtures of these two types of protein was measured because it is likely that the two would be present together in real food products.

Figure 5 illustrates the main types of behavior that were observed. Starting at bubble sizes between 100 and 200 μm, air bubbles stabilized by 1 wt % SC or BL dissolve away completely in approximately 120 min. Bubbles stabilized by 10^{-2} wt % HFBII kept their size indefinitely, i.e., over a time scale of at least a few days. Bubbles stabilized by 10^{-2} wt % HFBII + 0.3 wt % SC or 10^{-2} wt % HFBII + 0.3 wt % BL gave intermediate behavior, although the BL mixture gave more stable bubbles than the SC mixture. With both mixtures, however, the bubbles eventually slowly shrank and disappeared in a few hours. The results with the mixtures therefore suggest that, at the compositions used, both HFBII and milk proteins are present together at the bubble surface and that the milk proteins compromise the strength of the film formed by HFBII alone, presumably adding flexibility that allows for some bubble

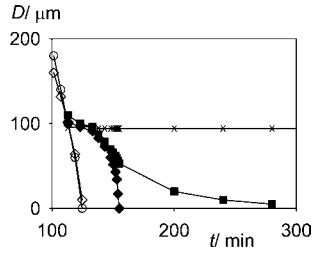

Figure 5. Shrinkage kinetics of single bubbles at the A–W interface. The bubble diameter (D) is plotted against time (t) for bubbles stabilized by 1 wt % SC (○), 1 wt % BL (◇), 0.3 wt % SC + 10^{-2} wt % HFBII (◆), 0.3 wt % BL + 10^{-2} wt % HFBII (■), and 10^{-2} wt % HFBII (×).

shrinkage. It is noticeable that, with the SC mixture, the time dependence of the shrinkage is similar to that of SC alone but more delayed, whereas with the BL mixture, the rate of shrinkage continually decreases. This is because SC is more surface-active than BL but less surface-active than HFBII (see the study by Cox et al.[5] and below). Thus, SC is more likely than BL to compete successfully with HFBII for adsorption sites at the interface, and therefore, with SC, the interfacial film is richer in SC than with BL and, consequently, has less resistance to shrinkage. When the bubbles shrink in the BL mixture, even if some BL is initially adsorbed, the BL is probably progressively displaced from the interface and the interfacial film becomes enriched in HFBII. Consequently, there is a large increase in resistance to shrinkage.

Surface Tension of Hydrophobin and Hydrophobin + Milk Proteins. Figure 6 shows the mean time-dependent

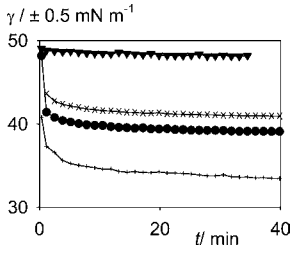

Figure 6. Surface tension (γ) versus adsorption time (t) for 10^{-3} wt % HFBII (×), 10^{-3} wt % HFBII + 0.5 mol dm^{-3} NaSCN (+), 10^{-2} wt % HFBII (●), and 0.04 wt % SC (▼). Each data point is the average of three sets of experimental results, with the error bars equal to the maximum variation about the mean.

surface tension values (γ) for HFBII at the same C_b as for the bubble stability experiments ($C_b = 10^{-2}$ wt %), as well as data for a lower C_b (10^{-3} wt %). The equilibrium γ values for 10^{-3} and 10^{-2} wt % HFBII are similar to those reported previously by Cox et al.[5] Increasing the HFBII concentration from $C_b = 10^{-3}$ to 10^{-2} wt % diminishes γ slightly. Including 0.5 mol dm^{-3} NaSCN with 10^{-3} wt % HFBII produces a more rapid and slightly more extensive lowering of γ than with 10^{-2} wt % HFBII alone, i.e., a 40 min value approximately 5 mN m^{-1} lower than for the latter. This is possibly due to the NaSCN helping to break up HFBII multimers in solution. The lower molecular weight species should diffuse more rapidly to the interface and pack more efficiently once adsorbed. These data suggest that the rate-limiting step for the adsorption of HFBII to the A–W interface is not the diffusion of the tetramer to the interface but the rate of dissociation of the tetramer at the

dx.doi.org/10.1021/jf304603m | J. Agric. Food Chem. 2013, 61, 1554–1562

interface. At C_b = 0.04 wt %, SC does not give an equilibrium γ as low as with a 40 times lower concentration of HFBII (i.e., C_b = 10^{-3} wt %), highlighting the much higher surface activity of HFBII.[5,10,40] However, for 0.04 wt % SC, the value of γ initially falls more rapidly than for 10^{-3} or 10^{-2} wt % HFBII, suggesting that, under these conditions, it takes more time to establish complete coverage of the interface with HFBII. This is in agreement with the results of the disproportionation measurements for the mixture of SC + HFBII, which suggested that at least some co-adsorption of SC occurs in the presence of 10^{-2} wt % HFBII. It also agrees with the relative difficulty of obtaining stable bubbles by injection under quiescent conditions with HFBII alone, e.g., for the coalescence measurements.

Surface Shear Viscosity (η_s). The mean values of surface shear viscosity (η_s) measured are shown in Figure 7. The results

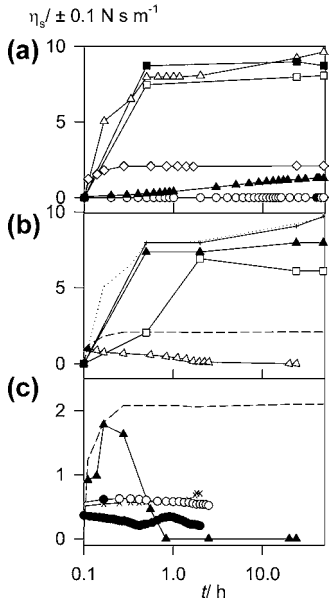

Figure 7. Surface shear viscosity (η_s) versus adsorption time (t) for various systems: (a) 10^{-2} wt % HFBII (△), 10^{-3} wt % BL (▲), 10^{-2} wt % BL (◇), 1 wt % SC (○), 10^{-2} wt % HFBII + 0.3 wt % BL (■), and 10^{-2} wt % HFBII + 0.3 wt % SC (□). (b) Showing the effect of 0.5 mol dm^{-3} NaSCN, 10^{-2} wt % HFBII + NaSCN (+), 10^{-2} wt % HFBII + 0.3 wt % SC + NaSCN (▲), 10^{-2} wt % HFBII + 1 wt % SC + NaSCN (□), and 10^{-2} wt % BL + NaSCN (△). The results for 10^{-2} wt % BL and HFBII on their own from panel a are indicated by the dashed and dotted lines, respectively. (c) Showing the effect of urea or SDS, 10^{-3} wt % HFBII alone (×), 10^{-3} wt % HFBII + 6 mol dm^{-3} urea (●), 10^{-3} wt % HFBII + 10^{-3} wt % SDS (○), and 10^{-2} wt % BL + 6 mol dm^{-3} urea (▲). The results for 10^{-2} wt % BL alone from panel a are indicated by the dashed line. Each data point is the average of three sets of experimental results, with the error bars equal to the maximum variation about the mean. Note that the time scale is the same on panels a, b, and c. The η_s scale is the same on panels a and b but shorter on panel c.

confirm the high η_s for HFBII alone,[10,22] higher than for SC or BL. Measurements (not shown) for up to 1 wt % SC do not give values of η_s significantly higher than those shown for 10^{-3} wt % SC, which are typically <10^{-2} N s m^{-1}, even after several hours of adsorption. Blijdenstein et al.[34] also compared the surface shear moduli of spread monolayers of HFBII, BL, and pure β-casein (which is the dominant surface-active component of SC) using a similar biconical geometry undergoing oscillations and found similar differences in magnitude for these three proteins. Upon the addition of a 30 times higher concentration (i.e., C_b = 0.3 wt %) of BL to 10^{-2} wt % HFBII, η_s is <1 N s m^{-1} higher at short (<2 h) adsorption times and <2 N s m^{-1} lower at long (>20 h) adsorption times, whereas for 0.3 wt % SC + 10^{-2} wt % HFBII at all adsorption times η_s is about 10% lower than for 10^{-2} wt % HFBII alone. These η_s results are in agreement with the coalescence measurements at the same compositions, where the low concentration of HFBII added to BL gave a slight increase in bubble stability compared to BL alone, which might be attributed to a stronger interfacial film, whereas there was only slight improvement upon the addition of HFBII to SC. On the other hand, HFBII alone gave poor coalescence stability, even though η_s was even higher. This points to the need for adsorbed films that are sufficiently strong but also sufficiently flexible to prevent coalescence when the interfacial film is suddenly deformed.[24,26,28,42] The η_s results are also in qualitative agreement with the disproportionation measurements for the same mixtures, where the results for the SC + HFBII combination suggest a significant weakening of the film that eventually allowed for complete shrinkage, while at short time the BL + HFBII combination allowed for shrinkage, but at longer time the resistance to shrinkage increased. The η_s measurements therefore seem to be sensitive to subtle changes in the composition and/or strength of the mixed films and how this effects stability to the different rates and types of deformation that occur during coalescence and disproportionation. At present, it has not been possible to quantify the interfacial composition of the protein layer in these mixed hydrophobin + milk protein films, although the neutron reflectivity techniques as used by Penfold et al.[43] might be able to do this in the future. In some respects, the results for the mixtures of HFBII + the milk proteins are similar to the findings by Parkinson et al.,[44] where it was shown that a low proportion (1% of the total protein present) of a more surface-active protein (in their case, casein) in a protein mixture could almost completely dominate the interfacial properties and corresponding emulsion stability, where the main protein constituent (in their case, whey protein) was slightly less surface-active.

The high η_s of globular proteins, such as BL, is often ascribed to their unfolding and cross-linking at the interface.[29] This makes the higher η_s for HFBII surprising, because HFBII molecules appear to undergo very little conformational change upon adsorption,[35] partly because the four internal disulfide cross-links maintain a very compact and rigid structure. Because hydrophobic forces are involved in the self-assembly of HFBII molecules in the bulk, one possibility is that hydrophobic forces are involved in the formation of the very strong films of HFBII at the A−W interface. To test this, η_s was also measured in the presence of NaSCN. The results in Figure 7b show that there was no significant effect on η_s of adding 0.5 mol dm^{-3} NaSCN to 10^{-2} wt % HFBII alone and a slight (1−2 N s m^{-1}) lowering of η_s upon addition to the mixture of 10^{-2} wt % HFBII + 0.3 wt % SC. This is in stark contrast to the effect of 0.5 mol dm^{-3} NaSCN on an adsorbed film formed from 10^{-2} wt % BL, which shows a reduction to zero η_s over a few hours, as also shown in Figure 7b. These results suggest that, at this macroscopic A−W interface, it is not hydrophobic bonding between HFBII molecules that confers the high surface shear viscosity of HFBII alone nor is there hydrophobic bonding between HFBII and SC at the interface. It should also be noted that the inclusion of NaSCN slightly lowers the final equilibrium γ of HFBII alone

(see Figure 6), which was interpreted as resulting from changes in the bulk aggregation of the protein rather than changes directly at the interface.

Figure 7b also shows the results of an experiment conducted using a higher C_b of SC (1 wt %) in combination with 10^{-2} wt % HFBII and 0.5 mol dm^{-3} NaSCN. The measured η_s did not rise so quickly, and the final value (after >24 h) was significantly (3−4 N s m^{-1}) lower than with 10^{-2} wt % HFBII alone. However, given that the bulk concentration of SC was 100 times that of HFBII, it is still surprising that the observed η_s is so high. Clearly, significant HFBII must persist at the interface, because the η_s of SC alone is very low in comparison (see Figure 7a). Radulova et al.[40] and Burke et al.[41] have recently investigated the surface shear viscosity of mixtures of pure β-casein + HFBII and concluded that the behavior is dominated by HFBII at even higher ratios of β-casein to HFBII.

Because hydrophobic bonding between HFBII molecules apparently cannot explain the high values of η_s, the effect of adding the hydrogen-bond-breaking agent urea to $C_b = 10^{-3}$ wt % HFBII was also tested. The results are shown in Figure 7c. In this case, 6 mol dm^{-3} urea also lowered η_s by approximately 0.5 N s m^{-1}, whereas the effect on an adsorbed film formed from 10^{-2} wt % BL was to lower η_s to zero in less than 2 h, similar to the effect of 0.5 mol dm^{-3} NaSCN on the same protein (see Figure 7b). Thus, neither does intermolecular hydrogen bonding seem to be required to give high η_s for adsorbed films of HFBII. One further experiment to test the resilience of the HFBII films was conducted. A mixed solution of 10^{-3} wt % SDS + 10^{-3} wt % HFBII was formed, and η_s was measured. The SDS produced virtually no change in the values of η_s for 10^{-3} wt % HFBII alone, despite being present at a SDS/HFBII mole ratio of >20:1. Such a concentration would normally completely destroy the surface viscoelasticity of any other globular protein,[45] but the result is in agreement with the neutron reflectivity studies by Zhang et al.,[19,20] who showed that SDS does not desorb HFBII until the critical micelle concentration (≈0.2 wt %) of SDS is exceeded. It seems that there are no obvious types of intermolecular bonds that are responsible for the high strength of the adsorbed HFBII films.

Surface Dilatational Elasticity (ε^*_{init}). The surface dilatational behavior of selected systems was also investigated. The dilatational response of the films should be thought particularly relevant to the results of the pressure-drop-induced coalescence experiments, where coalescence is initiated by film expansion. However, surface dilatational rheology is also relevant to resistance to disproportionation, which involves a decrease in the interfacial area. Figure 8 shows the average initial elasticity, ε^*_{init}, for 5×10^{-3} and 10^{-2} wt % HFBII as a function of the rate of area strain, d ln A/dt. The values of ε^*_{init} for 10^{-2} wt % HFBII are approximately half the values for 5×10^{-3} wt % HFBII at the slower speeds of expansion, as expected because of faster adsorption of protein from the bulk at higher C_b, thereby reducing $\Delta\gamma$. At the highest strain rate, the ε^*_{init} values converge to the same intermediate value ($\varepsilon^*_{init} \approx 60$ mN m^{-1}). The strain rate 0.07 s^{-1} corresponds to the rate of expansion in the pressure-drop coalescence tests, but it is seen that between 0.007 and 0.35 s^{-1}, the variation of ε^*_{init} with strain rate is minor. This is in agreement with similar measurements[24,26] on BL and SC and the general observation with several other protein systems[23,26] that bubble coalescence on pressure drop is more strongly correlated with the amount of expansion and not the rate of expansion for this range of rates and extents of bubble expansion. The high values of ε^*_{init},

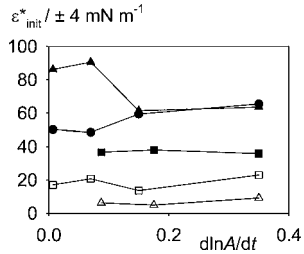

Figure 8. Average initial dilatational elasticity (ε^*_{init}) as a function of the surface expansion strain rate (d ln A/dt) for HFBII and mixtures with milk proteins. Data are shown for 5×10^{-3} wt % HFBII (▲), 10^{-2} wt % HFBII (●), 10^{-2} wt % HFBII + 0.3 wt % SC (□), 1 wt % SC (△), and 1 wt % BL (■). Each data point is the average of three sets of experimental results, with the error bars equal to the maximum variation about the mean.

i.e., large $\Delta\gamma$, upon expansion for HFBII are significant compared to the behavior of BL or SC under similar conditions[33] at all strain rates investigated. This probably relates to the relatively slow adsorption of HFBII aggregates and/or the slow interfacial redistribution of HFBII molecules upon expansion compared to other proteins, such as SC or BL, even though the final equilibrium γ is lower with HFBII.

Measurements of ε^*_{init} were also made for some of the protein mixtures, but because HFBII is far more surface-active than BL, while SC can apparently compete with HFBII for adsorption sites to some extent, measurements were confined to mixtures of HFBII and the latter protein. Figure 8 shows ε^*_{init} as a function of the strain rate for the mixed system of 10^{-2} wt % HFBII + 0.3 wt % SC. It is seen that ε^*_{init} is much lower for 1 wt % SC, because of the faster adsorption and rearrangement of adsorbed SC at this relatively high C_b. Although the concentration of SC in the mixed system is approximately 3 times lower, the behavior of ε^*_{init} in the mixture is closer to that of 1 wt % SC than 10^{-2} wt % HFBII. This in contrast to the surface shear viscosity results, where at this composition, η_s is still almost the same as HFBII on its own. The ε^*_{init} measurement probes protein adsorption kinetics upon an increase in surface area, while the η_s measurement is at a fixed area. Thus, the low ε^*_{init} values for the SC + HFBII mixture tend to point to some weakening of the film that agrees with the tendency for bubble shrinkage to occur (Figure 5), because for a purely elastic film, bubble shrinkage should cease if the dilatational elasticity is $>\gamma/2$ and bubbles shrink even faster when the elasticity is lower.[39] Recently, Radulova et al.[40] and Burke et al.[41] found that the dilatational moduli of HFBII tended to be largely unaffected by the addition of pure β-casein at pH 7. However, the highest concentration of β-casein used (ca. 0.1 wt %) was not as high as the concentrations of SC used here.

Blijdenstein et al.[34] point out that, with regard to resistance to disproportionation, the more relevant rheological measurement should be interfacial compression, and their own measurements of resistance to compression of spread protein monolayers confirm that dilatational elasticity > $\gamma/2$ only holds for HFBII. However, the high values of η_s measured here also point to a strengthening of the film that agrees with a definite increase in resistance to bubble shrinkage and also to an increase in resistance to bubble coalescence upon expansion. Blijdenstein et al.[34] also showed in their systems that the increased resistance to shrinkage/disproportionation also correlated with the higher surface shear moduli measured.

Thus, for the mixtures, there is more of a correlation of high η_s values with high bubble stability than with high dilatational rheology, as measured by the ε^*_{init} parameter. A similar strong connection between η_s and bubble coalescence has been observed upon addition of a low volume fraction of stable emulsion droplets to foams stabilized by BL and SC,[24,28] where the droplets also have the tendency to strengthen the adsorbed layer. Similarly, surface-active cellulose particles and also surface-active starch granule fragments have been shown to increase the surface shear viscoelasticity of adsorbed SC films, with concomitant increases in bubble and oil-in-water (O/W) emulsion stability.[45,46] Another natural class of food particulate materials capable of producing stable emulsions is the flavonoids,[47] but these have yet to be studied in conjunction with proteins.

In summary, at low HFBII concentrations (10^{-2} wt %), HFBII gives marginal improvement in the stability of bubbles in systems at much higher SC concentrations, but slightly greater improvement in stability is obtained upon adding HFBII to BL. This probably reflects the greater surface activity of SC compared to BL, meaning that SC is slightly better at competing with HFBII for the interface, although HFBII is still more surface-active overall. The stabilizing activity derived from HFBII is most likely due to its ability to form strong intermolecular interactions, as reflected in very high surface shear viscosity values measured. The more rapidly adsorbing milk proteins provide better bubble coalescence stability under a sudden pressure drop at short time scales, while HFBII provides enhanced strength over longer time scales, such as during disproportionation under quiescent conditions. The same considerations may also help to explain the capacity for hydrophobin to lead to high bubble stability and the phenomenon of "gushing" in the presence of other proteins and surface-active species in beers.[48]

However, important questions remain unanswered concerning the origins of the high film strength provided by HFBII, because the addition of agents that break hydrophobic bonds or hydrogen bonds do not seem to affect the film strength significantly. Although the hydrophobic patch of HFBII is the likely origin of its high surface activity at the A–W interface, no obvious attractive interactions between the adsorbed molecules can be detected, so that we tentatively suggest that the adsorbed HFBII molecules form a layer of rigid interlocking anisotropic Janus particles. If the molecules adsorb strongly and neatly interlock together to form a dense monolayer, the rigidity of the individual molecules will result in a high resistance to shear and, therefore, a high surface shear viscosity. However, because there are no attractive forces between the adsorbed HFBII molecules, the interfacial jamming may provide little resistance to expansion of the adsorbed film, as reflected in the bubble coalescence tests when the pressure is suddenly dropped and the lack of evidence for lateral interactions between HFBII molecules in monolayers. At the same time, a very strong adsorption energy of the molecules will resist their desorption upon compression, explaining the high resistance to disproportionation of bubbles. The coarse-grained molecular dynamics simulations of HFBII adsorption by Cheung[49] also suggest HFBII as a Janus nanoparticle, with a high desorption barrier of $80-120k_BT$, particularly if one eliminates protein flexibility. However, further work is required on the detailed structure and mechanics of adsorbed HFBII layers to prove the existence of this proposed interlocking or jamming of the molecules.

■ ASSOCIATED CONTENT

Supporting Information

A similar BAM image sequence as in Figure 2 but for a 22-h-old film adsorbed from $C_b = 10^{-2}$ wt % HFBII. This material is available free of charge via the Internet at http://pubs.acs.org.

■ AUTHOR INFORMATION

Corresponding Author

*Telephone: +44-0-113-343-2962. Fax: +44-0-113-343-2982. E-mail: b.s.murray@leeds.ac.uk.

Funding

This research was kindly supported by Unilever Research and Development and the Biotechnology and Biological Sciences Research Council (BBSRC) (Grant BBS/B/0501X).

Notes

The authors declare no competing financial interest.

■ REFERENCES

(1) Dickinson, E. In *Colloidal Particles at Interfaces*; Binks, B. P., Horozov, T. S., Eds.; Cambridge University Press: Cambridge, U.K., 2006; pp 298–327.

(2) Dickinson, E. Food emulsions and foams: Stabilization by particles. *Curr. Opin. Colloid Interface Sci.* **2010**, *15*, 40–49.

(3) Horozov, T. S. Foams and foam films stabilised by solid particles. *Curr. Opin. Colloid Interface Sci.* **2008**, *13*, 134–140.

(4) Murray, B. S. Stabilization of bubbles and foams. *Curr. Opin. Colloid Interface Sci.* **2007**, *12*, 232–241.

(5) Cox, A. R.; Cagnol, F.; Russell, A. B.; Izzard, M. J. Surface properties of class II hydrophobins from *Trichoderma reesei* and influence on bubble stability. *Langmuir* **2007**, *23*, 7995–8002.

(6) Linder, M. B. Hydrophobins: Proteins that self assemble at interfaces. *Curr. Opin. Colloid Interface Sci.* **2009**, *14*, 356–363.

(7) Kallio, J. M.; Linder, M. B.; Rouvinen, J. Crystal structures of hydrophobin HFBII in the presence of detergent implicate the formation of fibrils and monolayer films. *J. Biol. Chem.* **2007**, *282*, 28733–28739.

(8) Scholtmeijer, K.; Rink, R.; Hektor, H. J.; Wösten, H. A. B.; Dilip, K. A. Expression and engineering of fungal hydrophobins. In *Applied Mycology and Biotechnology*; Arora, D. K., Berka, R. M., Eds.; Elsevier: Amsterdam, The Netherlands, 2005; pp 239–255.

(9) Sarlin, T.; Nakari-Setala, T.; Linder, M. B.; Penttila, M.; Haikara, A. Fungal hydrophobins as predictors of the gushing activity of malt. *J. Inst. Brew.* **2005**, *111*, 105–111.

(10) Cox, A. R.; Aldred, D. L.; Russell, A. B. Exceptional stability of food foams using class II hydrophobin. *Food Hydrocolloids* **2009**, *23*, 366–376.

(11) Hakanpaa, J.; Linder, M.; Popov, A.; Schmidt, A.; Rouvinen, J. Hydrophobin in detail: Ultrahigh-resolution structure at 0.75 Å. *Acta Crystallogr., Sect. D: Biol. Crystallogr.* **2006**, *62*, 356–367.

(12) Kisko, K.; Szilvay, G. R.; Vuorimaa, E.; Lemmetyinen, H.; Linder, M. B.; Torkkeli, M.; Serimaa, R. Self assembled films of hydrophobin proteins HFBI and HFBII studied in situ at the air/water interface. *Langmuir* **2009**, *25*, 1612–1619.

(13) Butko, P.; Buford, J. P.; Goodwin, J. S.; Stroud, P. A.; McCormick, C. L.; Cannon, G. C. Spectroscopic evidence for amyloid-like interfacial self-assembly of hydrophobin Sc3. *Biochem. Biophys. Res. Commun.* **2001**, *280*, 212–215.

(14) Linder, M. B.; Szilvay, G. R.; Nakari-Setälä, T.; Penttilä, M. E. Hydrophobins: The protein amphiphiles of filamentous fungi. *FEMS Microbiol. Rev.* **2005**, *29*, 877–896.

(15) Lumsdon, S. O.; Green, J.; Stieglitz, B. Adsorption of hydrophobin proteins at hydrophobic and hydrophilic interfaces. *Colloids Surf., B* **2005**, *44*, 172–178.

(16) MacKay, J. P.; Matthews, J. M.; Winefield, R. D.; MacKay, L. G.; Haverkamp, R. G.; Templeton, M. D. The hydrophobin EAS is largely

unstructured in solution and functions by forming amyloid-like structures. *Structure* **2001**, *9*, 83−91.
(17) Szilvay, G. R.; Nakari-Setälä, T.; Linder, M. B. Behavior of *Trichoderma reesei* hydrophobins in solution: interactions, dynamics, and multimer formation. *Biochemistry* **2006**, *45*, 8590−8598.
(18) Basheva, E. S.; Kralchevsky, P. A.; Christov, N. C.; Danov, K. D.; Stoyanov, S. D.; Blijdenstein, T. B. J.; Kim, H.-J.; Pelan, E. G.; Lips, A. Unique properties of bubbles and foam films stabilized by HFBII hydrophobin. *Langmuir* **2011**, *27*, 2382−2392.
(19) Zhang, X. L.; Penfold, J.; Thomas, R. K.; Tucker, I. M.; Petkov, J. T.; Bent, J.; Cox, A.; Campbell, R. A. Adsorption behavior of hydrophobin and hydrophobin/surfactant mixtures at the air−water interface. *Langmuir* **2011**, *27*, 11316−11323.
(20) Zhang, X. L.; Penfold, J.; Thomas, R. K.; Tucker, I. M.; Petkov, J. T.; Bent, J.; Cox, A.; Grillo, I. Self-assembly of hydrophobin and hydrophobin/surfactant mixtures in aqueous solution. *Langmuir* **2011**, *27*, 10514−10522.
(21) Tchuenbou-Magaia, F. L.; Norton, I. T.; Cox, P. W. Hydrophobins stabilised air-filled emulsions for the food industry. *Food Hydrocolloids* **2009**, *23*, 1877−1885.
(22) Szilvay, G. R.; Paananen, A.; Laurikainen, K.; Vuorimaa, E.; Lemmetyinen, H.; Peltonen, J.; Linder, M. B. Self-assembled hydrophobin protein films at the air−water interface: Structural analysis and molecular engineering. *Biochemistry* **2007**, *46*, 2345−2354.
(23) Murray, B. S.; Dickinson, E.; Gransard, C.; Söderberg, I. Effect of thickeners on the coalescence of protein-stabilized air bubbles undergoing a pressure drop. *Food Hydrocolloids* **2006**, *20*, 114−123.
(24) Murray, B. S.; Cox, A. R.; Dickinson, E.; Nelson, P. V.; Wang, Y. Coalescence of expanding bubbles: Effects of protein type and included oil droplets. In *Food Colloids: Self-Assembly and Material Science*; Dickinson, E., Leser, M. E., Eds.; Royal Society of Chemistry: Cambridge, U.K., 2007; pp 369−382.
(25) Bailey, M. J.; Askolin, S.; Horhammer, N.; Tenkanen, M.; Linder, M.; Penttila, M.; Nakari-Setala, T. Process technological effects of deletion and amplification of hydrophobins I and II in transformants of *Trichoderma reesei*. *Appl. Microbiol. Biotechnol.* **2002**, *58*, 721−727.
(26) Murray, B. S.; Dickinson, E.; Lau, C. K.; Nelson, P. V.; Schmidt, E. Coalescence of protein-stabilized bubbles undergoing expansion at a simultaneously expanding planar air−water interface. *Langmuir* **2005**, *21*, 4622−4630.
(27) Linder, M. B.; Szilvay, G. R.; Nakari-Setälä, T.; Soderlund, H.; Penttilä, M. Surface adhesion of fusion proteins containing the hydrophobins HFBI and HFBII from *Trichoderma reesei*. *Protein Sci.* **2002**, *11*, 2257−2266.
(28) Murray, B. S.; Dickinson, E.; Wang, Y. Bubble stability in the presence of oil-in-water emulsion droplets: Influence of surface shear versus dilatational rheology. *Food Hydrocolloids* **2009**, *23*, 1198−1208.
(29) Murray, B. S. Interfacial rheology of food emulsifiers and proteins. *Curr. Opin. Colloid Interface Sci.* **2002**, *7*, 426−431.
(30) Borbas, R.; Murray, B. S.; Kiss, E. Interfacial shear rheological behaviour of proteins in three-phase partitioning systems. *Colloids Surf., A* **2003**, *213*, 93−103.
(31) Xu, R.; Dickinson, E.; Murray, B. S. Morphological changes in adsorbed protein films at the air−water interface subjected to large area variations, as observed by Brewster angle microscopy. *Langmuir* **2007**, *23*, 5005−5013.
(32) Murray, B. S.; Xu, R.; Dickinson, E. Brewster angle microscopy of adsorbed protein films at air−water and oil−water interfaces after compression, expansion and heat processing. *Food Hydrocolloids* **2009**, *23*, 1190−1197.
(33) Murray, B. S.; Cattin, B.; Schuler, E.; Sonmez, Z. O. Response of adsorbed protein films to rapid expansion. *Langmuir* **2002**, *18*, 9476−9484.
(34) Blijdenstein, T.; de Groot, P.; Stoyanov, S. On the link between foam coarsening and surface rheology: Why hydrophobins are so different. *Soft Matter* **2010**, *6*, 1799−1808.
(35) Askolin, S.; Linder, M. B.; Scholtmeijer, K.; Tenkanen, M.; Penttilä, M.; De Vocht, M. L.; Wösten, H. A. B. Interaction and comparison of a class I hydrophobin from *Schizophyllum commune* and class II hydrophobins from *Trichoderma reesei*. *Biomacromolecules* **2006**, *7*, 1295−1301.
(36) Aumaitre, E.; Wongsuwarn, S.; Rossetti, D.; Hedges; Cox, A. R.; Vella, D.; Cicuta, P. A viscoelastic regime in dilute hydrophobin monolayers. *Soft Matter* **2012**, *8*, 1175−1183.
(37) Murray, B. S.; Campbell, I.; Dickinson, E.; Maisonneuve, K.; Nelson, P. V.; Söderberg, I. A novel technique for studying the effects of rapid surface expansion on bubble stability. *Langmuir* **2002**, *18*, 5007−5014.
(38) Wösten, H. A. B.; De Vocht, M. L. Hydrophobins, the fungal coat unravelled. *Biochim. Biophys. Acta, Rev. Biomembr.* **2000**, *1469*, 79−86.
(39) Dickinson, E.; Ettelaie, R.; Murray, B. S.; Du, Z. Kinetics of disproportionation of air bubbles beneath a planar air−water interface stabilised by food proteins. *J. Colloid Interface Sci.* **2002**, *252*, 202−213.
(40) Radulova, G. M.; Golemanov, K.; Danov, K. D.; Kralchevsky, P. A.; Stoyanov, S. D.; Arnaudov, L. N.; Blijdenstein, T. B. J.; Pelan, E. G.; Lips, A. Surface shear rheology of adsorption layers from the protein HFBII hydrophobin: Effect of added β-casein. *Langmuir* **2012**, *28*, 4168−4177.
(41) Burke, J.; Cox, A. R.; Petkov, J.; Murray, B. S. Interfacial rheology and stability of air bubbles stabilized by mixtures of hydrophobin and β-casein. *Food Hydrocolloids* **2012**, DOI: 10.1016/j.foodhyd.2012.11.026.
(42) Freer, E. M.; Yim, K. S.; Fuller, G. G.; Radke, C. J. Shear and dilatational relaxation mechanisms of globular and flexible proteins at the hexadecane/water interface. *Langmuir* **2004**, *20*, 10159−10167.
(43) Penfold, J.; Thomas, R. K.; Shen, H.-H. Adsorption and self-assembly of biosurfactants studied by neutron reflectivity and small angle neutron scattering: Glycolipids, lipopeptides and proteins. *Soft Matter* **2012**, *8*, 578−591.
(44) Parkinson, E. L.; Dickinson, E. Synergistic stabilization of heat-treated emulsions containing mixtures of milk proteins. *Int. Dairy J.* **2007**, *17*, 95−103.
(45) Murray, B. S.; Durga, K.; Yusoff, A.; Stoyanov, S. D. Stabilization of foams and emulsions by mixtures of surface active food-grade particles and proteins. *Food Hydrocolloids* **2011**, *25*, 627−638.
(46) Murray, B. S.; Durga, K.; de Groot, P. W. N.; Kakoulli, A.; Stoyanov, S. D. Preparation and characterization of the foam-stabilizing properties of cellulose−ethyl cellulose complexes for use in foods. *J. Agric. Food Chem.* **2011**, *59*, 13277−13288.
(47) Luo, Z.; Murray, B. S.; Yusoff, A.; Morgan, M. R. A.; Povey, M. J. W; Day, A. J. Particle-stabilizing effects of flavonoids at the oil−water interface. *J. Agric. Food Chem.* **2011**, *59*, 2636−2645.
(48) Shokribousjein, Z.; Deckers, S. M.; Gebruers, K.; Lorgouilloux, Y.; Baggerman, G.; Veraschtert, H.; Delcour, J. A.; Etieme, P.; Roch, J.-M.; Derdelinckx, G. Hydrophobins, beer foaming and gushing. *Cerevisia* **2011**, *32*, 85−101.
(49) Cheung, D. L. Molecular simulation of hydrophobin adsorption at an oil−water interface. *Langmuir* **2012**, *28*, 8730−8736.